Electrochemical Detection of Polyphosphate Accumulation by Phosphate Accumulating Organisms for Wastewater Treatment

By

Patrick “Davis” Cobb

July, 2024

Director of Thesis: Dr. Eli Hvastkovs

Major Department: Chemistry

Inorganic phosphates are a very common additive to fertilizers used in industrial agriculture. While these additions result in larger healthier crop yields the runoff from these macronutrients ends up within local water ecosystems. The discharge of phosphate to water systems can lead to eutrophication and long-term damage to the local environment. To treat phosphate, local wastewater treatment systems (WWTP) often use bacteria to remove phosphate from the water. These phosphate treatment organisms are termed phosphate accumulating organisms (PAO) and sequester phosphate by converting it into long chains of polyphosphate. The efficiency of this process can vary due to myriad factors; therefore, the ability to monitor if the biological processes are occurring normally is a significant WWTP need.

To this end, an electrochemical biosensor was developed using Layer-by-Layer (LbL) methodology to immobilize films containing *Pseudomonas putida*, a model PAO, to detect polyphosphate uptake following soluble phosphate exposure. The bacterial films were exposed to electroactive methylene blue and phosphate with electrochemical monitoring using square wave voltammetry to determine methylene blue reduction currents. Currents at several potentials (vs. SCE) increase as a function of phosphate exposure, which were significantly elevated in the presence of *P. putida* vs. *E. coli* films. ICP-MS was used to show that *P. putida* sequesters phosphorus in significantly higher amounts than *E. coli*, which shows that the electrochemical output is due to poly-P accumulation on the electrode surface. The sensor was challenged with

interfering ion solutions and at varying temperatures to model conditions that might be encountered at the WWTP. Overall, this study lays the groundwork for the eventual biosensor use to measure PAO health and function at WWTP.

Electrochemical Detection of Polyphosphate Accumulation by Phosphate Accumulating Organisms for Wastewater Treatment

A Thesis

Presented to the Faculty of the Department of Chemistry

East Carolina University

In Partial Fulfillment of the Requirements for the Degree

Master of Science in Chemistry

By

Patrick “Davis” Cobb

July, 2024

Director of Thesis: Eli G. Hvastkovs, Ph.D.

Thesis Committee Members

Erin K. Field, Ph.D.

Pingping Meng, Ph.D.

ACKNOWLEDGEMENTS

I wish to acknowledge Dr. Eli Hvastkovs for his amazing mentorship throughout my time at East Carolina University. I would also like to extend a large thank you to my Mother, for believing in me and pushing me forward in every stage of my life, and my brother, who has always been my best friend and my support raft.

TABLE OF CONTENTS

LIST OF FIGURES

LIST OF SYMBOLS AND ABBREVIATIONS

ATP	Adenine triphosphate
CV	Crystal Violet
DAPI	4', 6-diamidino-2-phylindole
DI	Deionized
DNA	Deoxyribose nucleic acid
E. coli	Escherichia coli
EBPR	Enhanced Biological Phosphate Removal
ESI-MS	Electrospray ionization-mass spectrometry
GUC	Greenville Utilities Commission
ICP-MS	Inductively coupled plasma-mass spectrometry
K_{sp}	Solubility product constant
LbL	Layer-by-layer
MB+	Methylene Blue
μg	Microgram
MS	Mass Spectrometry
mV	Millivolt
NMR	Nuclear magnetic resonance
P	Phosphorus
P. putida	*Pseudomonas putida*
PAO	Phosphate accumulating organisms
PDDA	Poly(diallydimethylammonium chloride)
PHA	Polyhydroalkanoates
PO_4^{3-}	Phosphate
Poly-P	Polyphosphate
ppb	Parts per billion
PSS	Poly(3,4-ethylenedioxythiophene) polystyrene sulfonate
RPM	Rotations per minute
SCE	Saturated Calomel Electrode
SWV	Square Wave Voltammetry
USGS	United States Geological Survey
WWTP	Wastewater Treatment Plants
WWTS	Wastewater Treatment Systems
μM	Micromolar

CHAPTER 1: INTRODUCTION AND BACKGROUND

1.1 Phosphate in the Environment

The anthropogenic addition of phosphorus to the environment is a key concern. The most notable sources of phosphorus come from phosphate (PO_4^{3-}) released into the environment from industrial agriculture. PO_4^{3-} is a common additive to fertilizers, along with nitrogen and potassium.[1, 2, 3] These macronutrients are vital for large plant growth and enhance soil characteristics to increase crop yields.[5] Macronutrients that are not absorbed by the crops are subject to runoff from rain and irrigation and end up in local water reservoirs.[1, 4]

In water systems, PO_4^{3-} is a limiting reagent for microbial growth; therefore, increases in PO_4^{3-} cause bacterial growth, which can lead to eutrophication in lakes, rivers, and coastal zones. During eutrophication, colonies of cyanobacteria and other types of phytoplankton quickly dominate the local ecosystem. The phytoplankton eventually sink, die, and decompose, removing oxygen present in the water system, starving all other organisms, and resulting in a significant decrease of life within the ecosystem.[5] Even when this process plays out on a minor scale, the ecosystem can be irreversibly altered from primarily featuring benthic microalgae and macrophytes transitioning to one dominated by phytoplankton. This change reduces both fish production efficiency and the biodiversity of autotrophs and heterotrophs while increasing the production of various greenhouse gases such as methane and nitrous oxide.[4]

1.2 Wastewater Treatment with Phosphate Accumulating Organisms

To preclude such environmental disasters, Wastewater Treatment Systems (WWTS) in local municipalities are tasked with treating these nutrients, including PO_4^{3-}. According to the United States Geological Survey (USGS), in 2015 the United States consumed 322 billion gallons of water per day from both saline (41 billion gallons) and freshwater sources (281 billion gallons), with much of this water going to thermoelectric power and irrigation, which is shown in Figure 1.1.[7]

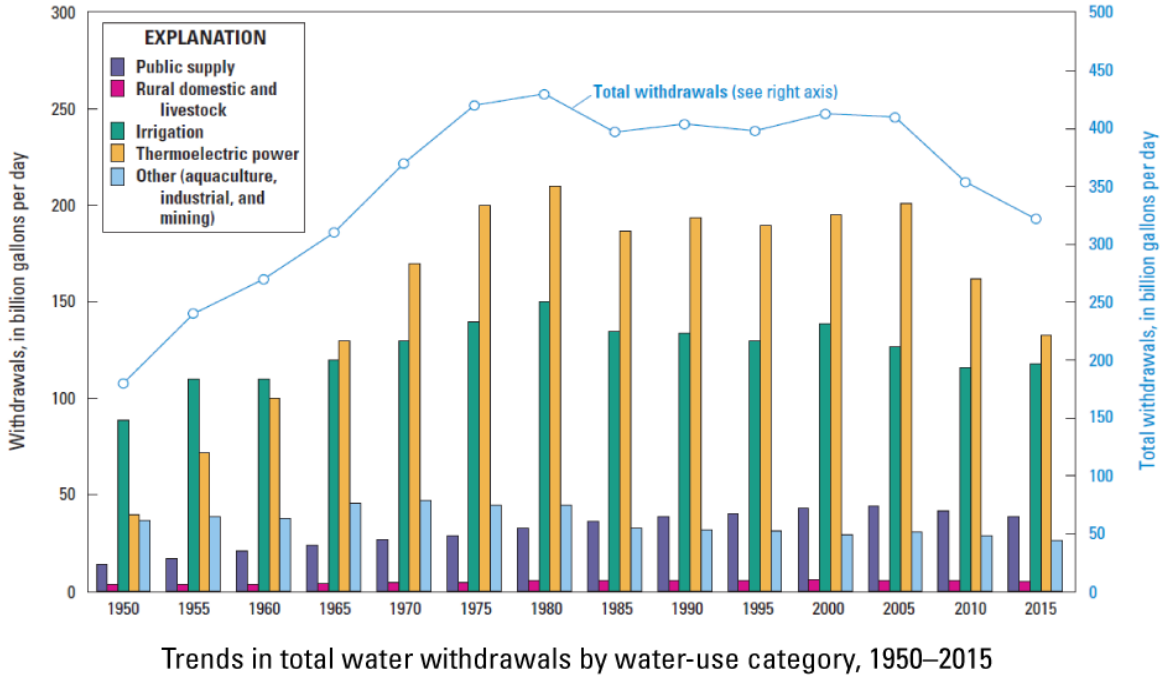

Figure 1.1. Detailed chart showing of United States water usage from 2050-2015 Credit USGS

Despite recent trends of more efficient water usage as evidenced from the plateau and decline in overall water withdrawal in Figure 1.1, billions of gallons of water used every day must still be treated before environmental discharge. This must be performed in ways that are mindful to both the environment and economic matters.[4,5,6]

One such way WWTP performs this task is through Enhanced Biological Phosphate Removal (EBPR), which is the primary method for the removal of PO_4^{3-} from wastewater as compared to chemical based removal in primary treatment or filter based removal in tertiary treatment.[3,4] This process exploits the use of phosphate accumulating organisms (PAOs), a collection of bacterial organisms that store inorganic PO_4^{3-} as long polyphosphate (poly-P) chains under aerobic conditions.[1] Such organisms are often from genera *Tetraspaera* or *Pseudomonas* and store the poly-P in chains ranging from three to over 1000 of tetrahedral P units held together by high energy phosphoanhydride bonds.[3] These poly-P stores serve a wide range of cellular functions such as energy storage, formation of membrane channels for uptake of biomolecules, pH buffering, regulation of enzyme activity, stress responses and cation sequestration and storage.[2]

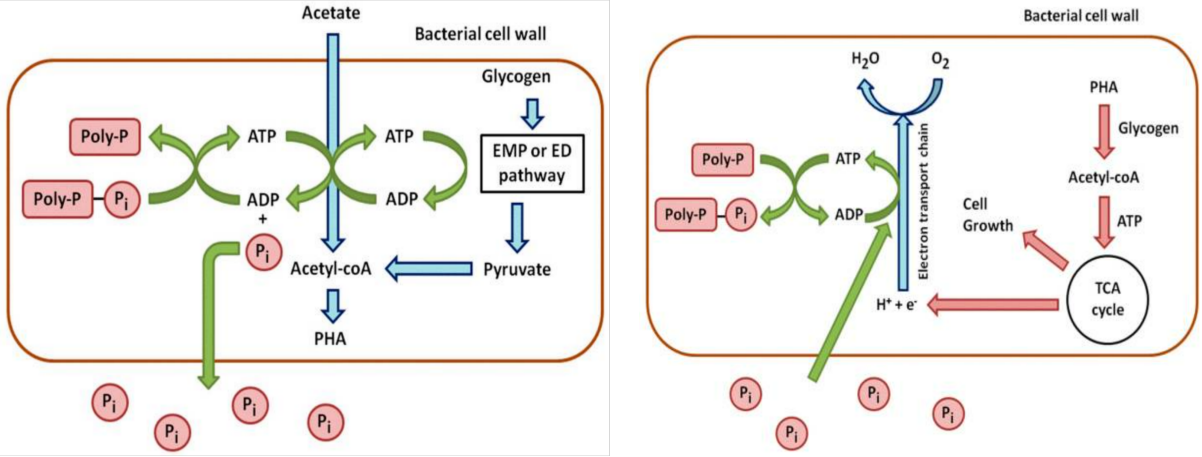

Figure 1.2. Scheme showing the pathways for both the anaerobic and aerobic phases of Enhanced Biological Phosphorous Removal. Credit: Cédric Tarayre, 2016[8]

Figure 1.2 shows the process of utilizing EBPR to treat PO_4^{3-} in wastewater. The PAOs in the EBPR tank are contained in an aerobic basin where oxygen levels can be controlled.[1,4,7] This allows the WWTP to control various metabolic processes that occur under both aerobic and anaerobic conditions.[1,4,9] The PAOs are initially subjected to oxygen starvation. This phase is

considered a stress condition for PAOs, which adapt by seeking carbon sources to cope with lack of oxygen. In wastewater, the most common sources of carbon are polyhydroalkanoates (PHAs) shown in left side of Figure 1.2.[1,8] Here bacteria break down any poly-P stores present within the bacteria and convert them into adenine triphosphate (ATP) for energy use and cell maintenance and combine them with acetyl-coA to form PHAs as a high source of carbon. During this process the bacteria release excessive phosphates into the system around them as monophosphate, or orthophosphate.[1,9]

During the next stage the tank is heavily oxygenated, which acts to reverse the initial starving process. PHAs are quickly consumed and metabolized initiating new cell growth. As the population of PAOs increase dramatically, the organisms begin luxury phosphate uptake, where soluble wastewater PO_4^{3-} can be accumulated and stored as poly-P, shown in the right side of Figure 1.2.[9] Here the PHAs are broken down and the components are quickly used for cell growth and converted into excess ATP which is used to build poly-P stores.[1,9]

EBPR is influenced by many different experimental conditions. It is well documented that temperatures higher than 30°C can cause other bacteria in the activated sludge, the culture of organisms developed in aerobic conditions,[9] to out-compete PAOs, preventing PO_4^{3-} accumulation.[10] pH conditions lower than 6.5 also foster an environment for competition among other bacteria and the PAO, while they remain more effective at their removal process at pH range 7-7.5.[10, 11]

1.3 Detection of Poly-P

There are a variety of methods for detecting and quantifying poly-P in PAOs. Direct detection techniques often involve staining with a variety of dyes such as toluidine blue or methylene blue with detection via light and epifluorescence microscopy.[9,12, 13] Other techniques such as flow cytometry can be used with 4', 6-diamidino-2-phylindole (DAPI) stain to locate specific pockets of poly-P inside PAO for eventual separation techniques.[9, 13]

Quantification of poly-P often involves their extraction from the PAOs using a variety of separation and extraction techniques as the first step. This often proves difficult due to poly-P integration into various cellular structures such as deoxyribose nucleic acid (DNA) and cell membranes.[1,9,12] Common methods of extraction involve either a sulfuric acid column based purification[14] or an enzymatic process using phosphate kinase and exopolyphosphatase.[9, 12] These techniques are used to convert poly-P into singular orthophosphate entities and then quantifying those units.[12, 15, 16, 17] Commonly, DAPI fluorescence or Raman spectroscopy are used to quantitate these individual units.[15, 16, 17]

Other methods do exist for measuring poly-P inside organisms without the need for extraction. For example, nuclear magnetic resonance (NMR) spectroscopy represents an option for non-invasive and non-destructive option for labeled ^{31}P substrates. This can give an overview of all molecules that contain phosphorus, including poly-P, monophoshphate, diphosphate and other types of cellular phoshorus.[9, 17] Though NMR is used to show relative abundance of poly-P in comparison to other phosphorus-bond classes like phosphoesters and phosphonates.[17]

Electrospray ionization-mass spectrometry (ESI-MS) is another useful technique that can be used for detection and quantification of poly-P without extraction. MS has powerful

advantages as it is a sensitive and highly selective technique. MS can be used to detect a high number of different analytes in a sample without pre-extraction and separation.[13, 17, 18] MS has been used to detect and quantify smaller poly-P structures, such as monophosphate, diphosphate, tripolyphosphate and tetrapolyphosphate.[18]

1.4 Electrochemical Detection Methods

Electrochemical methods represent an emerging set of techniques for analyzing poly-P in these types of wastewater mixtures. Many bio-electrochemical assays monitor the current output of a desired analyte that can provide information about a biologically relevant process as a function of the applied potential vs. a reference electrode. Generally, electrochemical methods are cost-effective, simple and highly sensitive techniques, which represent a promising alternative for phosphate and poly-P detection.[19] For instance, an amperometric assay employing a carbon electrode modified with electrocatalyst cobalt phthalocynanine and a cellulose acetate membrane has been used to quantitate PO_4^{3-} in urine with concentrations between 20-180 mM.[20] In environmental samples, screen-printed electrodes modified with electroactive phosphomolybdate and carbon black nanoparticles were used to detect PO_4^{3-} in water with concentrations as low as 6 mM using an amperometric (measuring current at an applied potential) strategy.[21]

An alternate approach to sensitive electrochemical detection is to employ square wave voltammetry (SWV).[22] SWV operates via a series of forward and backward potential pulses where the forward pulse is a few mV greater than the backward, resembling a sort of potential staircase. The current is monitored at both the back and forward pulses and typically plotted as

the difference.[22,23] The power of the technique comes from its speed compared to other differential methods, and plotting the difference current removes any non-Faradaic, or background, currents, which makes it a very sensitive option for detection.

1.5 – Sensor Construction Strategy and Experimental Goals

One of the main drawbacks to EBPR is that it is difficult to determine if the bacteria are operating efficiently to remove phosphate from the water. This process is impacted by several different conditions, many of which may be out of WWTP control, such as daily temperature. Regardless, knowledge of whether the EBPR process is operating normally, with the possibility of providing a quantitative output to the removal process, could provide a prospective WWTP with valuable information that can stave off expensive treatment options down the line.

To this end, the following chapters describe the initial development of a PAO electrochemical sensor to detect poly-P accumulation by PAO and provide some quantitative output to the process. At many WWTP, the types of bacteria operating in the EBPR process are not typically well known. Though most bacteria can accumulate phosphate, very few are dedicated PAOs. *Pseudomonas putida (P. putida)* is a known PAO and is found in many WWTP.[7] This bacterium was selected as the model PAO based on the ease at which it can be cultured and grown. These model PAO bacteria were immobilized on a graphite electrode via established layer-by-layer (LbL) methodology. LbL is a technique originally developed to organize proteins and other biomolecules or nanoparticles within layers of polymers of alternating charges. This process generates stable layers due to electrostatic forces between the alternating layers. Here, poly(diallydimethylammonium chloride) (PDDA) and poly(3,4-ethylenedioxythiophene) polystyrene sulfonate (PSS) were the underlying polymers used to

create the initial immobilization bed on the electrode surface. This process has been used to bind small cellular components, including DNA, and protein structures such as cytochrome P450 enzymes.[24, 25, 26] Many bacteria within EBPR exist in biofilm-forming communities. The biofilm generation fosters bacterial adherence to surfaces.[24] Utilizing this property, we have previously shown that similar bacterial colonies can be grown on an polymer modified electrode to measure biofilm destruction utilizing novel small-molecules and peptides.[27] A similar process was applied here, with the bacterial biofilm modified electrodes exposed to concentrations of PO_4^{3-} , but with alterations to the electrochemical output compared to our previous studies.

While our previous electrochemical studies utilized the electroactive compounds produced by *P. aeruginosa*, here we employed methylene blue (MB^+) as the electroactive indicator. Similar to aforementioned DAPI, MB^+ has been shown to penetrate poly-P stores within PAOs.[22] This molecule is electroactive and its reduction current can be easily monitored using SWV. As poly-P forms and/or is broken down within the bacteria, a corresponding change in MB^+ electrochemical potential occurs, which can provide information about the immobilized PAO and the poly-P storage process.

Once the experimental parameters to establish the bacteria on the electrode were optimized, the sensor was tested under applicable environmental conditions including environmentally relevant media that mimics environmental conditions, such as salt content and pH. Also, temperature of the media was altered to test the efficacy of the sensor to detect poly-P accumulation.

Finally, we attempted to validate the electrochemical sensor outputs utilizing mass spectrometry approaches, including inductively coupled plasma–mass spectrometry (ICP-MS). The electrochemical outputs simply report on the presence/absence of MB^+, but otherwise need

to be validated to ensure that the output was indeed based on PAO accumulation of poly-P. Also, the current outputs should provide some sort of quantitative output, which MS approaches can provide. ICP-MS is used primarily for elemental analysis and was effective in allowing us to monitor the ability of PAO removing phosphorus in the form of phosphate form from a solution.

Overall, the environmental effects of PO_4^{3-} discharge have been well documented, leading to population explosions of single cell organisms that have the potential to harm or lead to the destruction of ecosystems via eutrophication. Municipal WWTS use PAOs to remove PO_4^{3-} from local water systems by manipulating oxygen content within the wastewater facilities, causing PAOs to convert PO_4^{3-} into poly-P. Monitoring the health and activity of these bacteria is often a difficult task due to many environmental factors such as pH and temperature. Electrochemical biosensors may provide insight into the efficiency of the PAOs by allowing electroactive dyes to form reducible complexes with poly-P complexes within PAOs and their biofilms. This research lays the groundwork for the potential biosensor to monitor these processes in a real-world setting, which could eventually save WWTP plant operators and their water consumers time and money.

References

(1) Sheila M. Saia, Hunter J. Carrick, Anthony R. Buda, John M. Regan, and M. Todd Walter, *Critical Review of Polyphosphate and Polyphosphate Accumulating Organisms for Agricultural Water Quality Management*, Environmental Science & Technology 2021, 55(5), 2722-2742. DOI: 10.1021/acs.est.0c03566.

(2) Akbari A, Wang Z, He P, Wang D, Lee J, Han IL, Li G, Gu AZ. *Unrevealed roles of polyphosphate-accumulating microorganisms. Microb Biotechnol*. 2021, 14(1), 82-87. DOI: 10.1111/1751-7915.13730.

(3) Wurtsbaugh, WA, Paerl, HW, Dodds, WK. *Nutrients, eutrophication and harmful algal blooms along the freshwater to marine continuum*. WIRES. 2020, 6:e1373. DOI: 10.1002/wat2.1373.

(4) United States Geological Survey. *Total water use in the United States*, last revised June 2018. https://www.usgs.gov/special-topics/water-science-school/science/total-water-use-united-states#overview (accessed 2022-11-20).

(5) Bunce JT, Ndam E, Ofiteru, ID, Moore A, Graham D. W. *A Review of Phosphorus Removal Technologies and Their Applicability to Small-Scale Domestic Wastewater Treatment Systems,* Frontiers in Environmental Science. 2018, 22(6). DOI: 10.3389/fenvs.2018.00008.

(6) Environmental Protection Agency. *Agriculture Nutrient Management and Fertilizer,* last revised September 2022. https://www.epa.gov/agriculture/agriculture-nutrient-management-and-fertilizer (accessed 2022-11-20).

(7) Günther S, Trutnau M, Kleinsteuber S, Hause G, Bley T, Röske I, Harms H, Müller S. *Dynamics of polyphosphate-accumulating bacteria in wastewater treatment plant microbial*

communities detected via DAPI (4',6'-diamidino-2-phenylindole) and tetracycline labeling. Appl Environ Microbiol. 2009, 75(7), 2111-21. DOI: 10.1128/AEM.01540-08.

(8) Tarayre C, Nguyen HT, Brognaux A, Delepierre A, De Clercq L, Charlier R, Michels E, Meers E, Delvigne F. *Characterisation of Phosphate Accumulating Organisms and Techniques for Polyphosphate Detection: A Review*. Sensors. 2016, 16(6), 797. DOI: 10.3390/s16060797.

(9) Lopez-Vazquez CM, Oehmen A, Hooijmans CM, Brdjanovic D, Gijzen HJ, Yuan Z, van Loosdrecht MCM. *Modeling the PAO–GAO competition: Effects of carbon source, pH and temperature.* Water Research 2009, 43(2), 450–462. DOI: 10.1016/J.WATRES.2008.10.032.

(10) Filipe CD, Daigger GT, Grady CL. *Effects of pH on the Rates of Aerobic Metabolism of Phosphate-Accumulating and Glycogen-Accumulating Organisms*. Water Environment Research, 2001, 73, 213-222. DOI:10.2175/106143001X139201.

(11) Hupfer M, Glöss S, Schmieder P, Grossart, HP. *Methods for Detection and Quantification of Polyphosphate and Polyphosphate Accumulating Microorganisms in Aquatic Sediments*. International Review of Hydrobiology. 2009, 93, 1-30. DOI: 10.1002/iroh.200610935.

(12) Eixler S, Selig U, Karsten U. *Extraction and detection methods for polyphosphate storage in autotrophic planktonic organisms*. Hydrobiologia. 2005, 533, 135–143. DOI: 10.1007/s10750-004-2406-9.

(13) Werner TP, Amrhein N, Freimoser FM. *Novel method for the quantification of inorganic polyphosphate (iPoP) in saccharomyces cerevisiae shows dependence of iPoP content on the growth phase*. Archives of Microbiology. 2005, 184(2), 129-36. DOI: 10.1007/s00203-005-0031-2

(14) Kulakova AN, Hobbs D, Smithen M, Pavlov E, Gilbert JA, Quinn JP, McGrath JW. *Direct Quantification of Inorganic Polyphosphate in Microbial Cells Using 4'-6-Diamidino-2-Phenylindole (DAPI)*, Environmental Science & Technology. 2011, 45 (18), 7799-7803, DOI: 10.1021/es201123r.

(15) Moudříková S, Sadowsky A, Metzger S, Nedbal L, Mettler-Altmann T, Mojzeš P. *Quantification of Polyphosphate in Microalgae by Raman Microscopy and by a Reference Enzymatic Assay,* Analytical Chemistry. 2017, 89 (22), 12006-12013. DOI: 10.1021/acs.analchem.7b02393.

(16) Majed N, Li Y, Gu AZ. *Advances in techniques for phosphorus analysis in biological sources.* Current Opinion in Biotechnology, 2012, 23(6), 852–859. DOI: 10.1016/j.copbio.2012.06.002.

(17) Cobb SJ, Macpherson JV. *Enhancing Square Wave Voltammetry Measurements via Electrochemical Analysis of the Non-Faradaic Potential Window*, Analytical Chemistry. 2019, 91 (12), 7935-7942. DOI: 10.1021/acs.analchem.9b01857.

(18) Kabir MF, Rahman, MT Gurung A, Qiao Q. *Electrochemical Phosphate Sensors Using Silver Nanowires Treated Screen Printed Electrodes,* Sensors. 2018, 18(9), 3480-3485. DOI: 10.1109/JSEN.2018.2808163.

(19) Gilbert L, Jenkins AT, Browning S, Hart JP. *Development of an amperometric assay for phosphate ions in urine based on a chemically modified screen-printed carbon electrode*. Anal Biochem. 2009, 393(2), 242-7. DOI: 10.1016/j.ab.2009.06.038.

(20) Choi BK, Hercules DM, Houalla M. *Characterization of Polyphosphates by Electrospray Mass Spectrometry*, Analytical Chemistry. 2000, 72 (20), 5087-5091. DOI: 10.1021/ac000044q.

(21) Talarico D, Cinti S, Arduini F, Amine A, Moscone D, Palleschi G. *Phosphate Detection through a Cost-Effective Carbon Black Nanoparticle-Modified Screen-Printed Electrode Embedded in a Continuous Flow System*. Environmental Science & Technology. 2015, 49 (13), 7934-7939. DOI: 10.1021/acs.est.5b00218.

(22) Serafim LS, Lemos PC, Levantesi C, Tandoi V, Santos H, Reis MAM. *Methods for detection and visualization of intracellular polymers stored by polyphosphate-accumulating microorganisms*, Journal of Microbiological Methods. 2002, 51(1), 1-18. DOI:1016/S0167-7012(02)00056-8.

(23) López-Sánchez A, Leal-Morales A, Jiménez-Díaz L, Platero AI, Bardallo-Pérez J, Díaz-Romero A, Acemel RD, Illán JM, Jiménez-López J, Govantes F. *Biofilm formation-defective mutants in Pseudomonas putida*, FEMS Microbiology Letters. 2016, 363(13). DOI: 10.1093/femsle/fnw127.

(24) He P, Hu N, Rusling JF. *Driving Forces for Layer-by-Layer Self-Assembly of Films of SiO_2 Nanoparticles and Heme Proteins*. Langmuir. 2004, 20(3), 722–729. DOI: 10.1021/la035006r.

(25) Ma H, Hu N, Rusling JF. *Electroactive Myoglobin Films Grown Layer-by-Layer with Poly(styrenesulfonate) on Pyrolytic Graphite Electrodes*. Langmuir. 2000, 16(11), 4969–4975. DOI: 10.1021/la991296t.

(26) Lvov YM, Lu Z, Schenkman JB, Zu X, Rusling JF. *Direct Electrochemistry of Myoglobin and Cytochrome P450cam in Alternate Layer-by-Layer Films with DNA and Other Polyions.* Journal of the American Chemical Society. 1998, 120(17), 4073–4080. DOI: 10.1021/ja9737984.

(27) Robb AJ, Vinogradov S, Danell AS, Anderson E, Blackledge MS, Melander C, Hvastkovs EG., *Electrochemical detection of small molecule induced Pseudomonas aeruginosa biofilm dispersion*, Electrochimica Acta. 2018, 268, 276-282. DOI: 10.1016/j.electacta.2018.02.113.

CHAPTER 2: EXPERIMENTAL PROTOCOLS

2.1 Solutions

2.1.1 Polymer solutions and Electrochemical Buffer

Poly(diallydimethylammonium chloride) (PDDA) and poly(3,4-ethylenedioxythiophene) polystyrene sulfonate (PSS, Sigma Aldrich) solutions were prepared at a 6 mg mL^{-1} in deionized (DI) water containing 50 mM NaCl. These experiments were performed in a buffer consisting of 10mM Tris base (Sigma Aldrich) and 10mM NaCl in DI water (E-buffer) adjusted to pH 7.4 using hydrochloric acid.

2.1.2 Nutrient Broth

A nutrient broth was prepared by dissolving 8 g of Nutrient Broth mixture (Remel,REF R454202) in 1 L DI water before mixing well and sterilizing in an autoclave.

2.1.3 Bacteria and Biofilm Growth

Two separate 40% glycerol stocks of *Pseudomonas putida (P. putida,* Migula ATCC strain 12633*),* and *Escherichia coli DH5α, (E. coli)* were stored at -80ºC. 5 mL of nutrient broth was added to a 15 mL Falcon centrifuge tube which was inoculated with the individual bacteria strains using a sterile loop and allowed to grow for 48 hr at 200 RPM at 25ºC on a shaking incubator (Thermo). After this time, 1 mL of the resulting bacterial growth solution was added to 9 mL of nutrient broth and allowed to grow for an additional 12 hr in the shaking incubator at 200 RPM and 25º C. This was termed the working *P. putida* or *E. coli* solution.

2.2 Electrode preparation

Working electrodes were 6 mm dia. high purity graphite (HPG) electrodes polished sequentially using p800 and p300 grit SiC paper for 30 s each before sonication briefly to remove excess carbon. The electrodes were then rinsed with DI water dried under a stream of Ar.

These electrodes were then layered with the PDDA/PSS solutions in 20 µL aliquots for 15 min for each layer. The layering order was $(PDDA/PSS)_3PDDA$. After each layer 15 min exposure, the electrodes were rinsed with DI water. These layers provide a surface for bacterial biofilms to adhere more easily.

Once polymer layering was complete, the electrodes were placed into 250 µL of the working *P. putida* or *E. coli* solution in a 0.5 mL microcentrifuge tube. The tube was parafilmed and inverted. The bacteria were allowed to grow on the electrodes in an incubator at 200 rpm for 12 hr.

2.3 Electrochemical Assay

Electrochemical experiments were conducted employing a CH Instruments (Auston, TX) CHI 660A potentiostat with the bacteria modified graphite working electrode, a Pt counter electrode, and a saturated calomel electrode (SCE, saturated KCl) as reference. The SWV parameters for all experiments were: initial potential 1.2 V, final potential -0.9 V, incremental step 0.004 V, amplitude 0.025 V, frequency 15 Hz, quiet time 2s, sensitivity 1×10^{-3} A.

The bacteria modified electrodes were exposed to 1 µM methylene blue (MB^+) in 10mL E-buffer solution with SWV acquisition over 2 hr at specific times (0, 5, 10, 20, 40, 60, 120 min). Upon obtaining a stable SWV baseline, the bacteria modified/MB^+ equilibrated electrode

was exposed to sodium phosphate solutions (Sigma Aldrich) ranging between 0-500 μM with SWV acquisitions at specific time points over 2 hours (0, 3, 5, 10, 20, 40, 60, 120 min).

For biologically relevant solutions, concentrations of relevant ions were sourced from influent data provided by the Greenville Utilities Commission (GUC). 124 mg of calcium carbonate, 0.3072 mg of sodium nitrate, and 700 μL of ammonium hydroxide (from a 14.8 N stock) were dissolved in 1L of DI water with pH adjustment to 7.2 using 6 N HCl. These samples were subjected to a 1 μM MB^+ equilibration for 2 hr followed by exposure to 100 μM phosphate for 20 min. All reagents for this solution were either obtained from Sigma Aldrich or reagent grade.

2.4 Crystal Violet Assay

To assess biofilm content on the electrode surface, a modified crystal violet assay was performed. Electrodes were prepared as normal, but instead of being used in the electrochemical assay, they were exposed to a solution of 0.1% crystal violet in DI H_2O for 20 min after which they were rinsed with DI water and submerged in precisely 100μL of 35% acetic acid for an additional 1min. 50 μL of the resulting solution was pipetted into 1 cm pathlength quartz cuvettes and placed into a Varian Cary 300 Bio UV-Vis spectrophotometer. Visible absorption spectra were recorded using the following parameters: scan range 800.00nm - 400.00nm, ave time 0.100 s, data interval 1.000 nm, scan rate 600.000 nm min^{-1}.

2.5 ICP-MS

10 mL working bacteria solutions of both *E. coli* and *P. putida* were prepared in a 15 mL Falcon centrifuge tube and degassed with Ar for 60 min and allowed to rest for 2 hr. Following this rest time, phosphate standard was added to this solution to achieve a concentration of 5000

ppb (~166 μM), followed by perfusion with O_2 for 60 min. These samples were placed on a shaking incubator for 24 hr at 25º at 250 RPM. After 24 hr, these solutions were filtered through a centrifuge filter (Amicon Ultra 3000 mw cutoff, 5 mL total volume). 1 mL of this filtrate was diluted to 10 mL with DI water for a calculated phosphate concentration of 500 ppb. Prepared controls were nutrient broth with and without addition of 5000 ppb phosphate. Each was incubated and filtered following the same protocols before diluting 1:10 in DI water.

These samples, along with a series of standards (200, 400, 800, 1500 ppb phosphorus, HPS, ICP-AM-MISA-250, 100 μg mL^{-1}) were analyzed using ICP-MS using conditions: lens parameters extract: 2→-230V, He gas flow 5.0mL min^{-1}, omega bias -100V, omega lens 9.6V, deflect 1.0V. Data acquisition parameters: *m/z* isotopes monitored ^{31}P, *m/z* of internal standards ^{6}Li, ^{7}Li, ^{113}In, ^{115}In, ^{118}In.

CHAPTER 3: ELECTROCHEMICAL ASSAY

3.1 Biofilm Assay

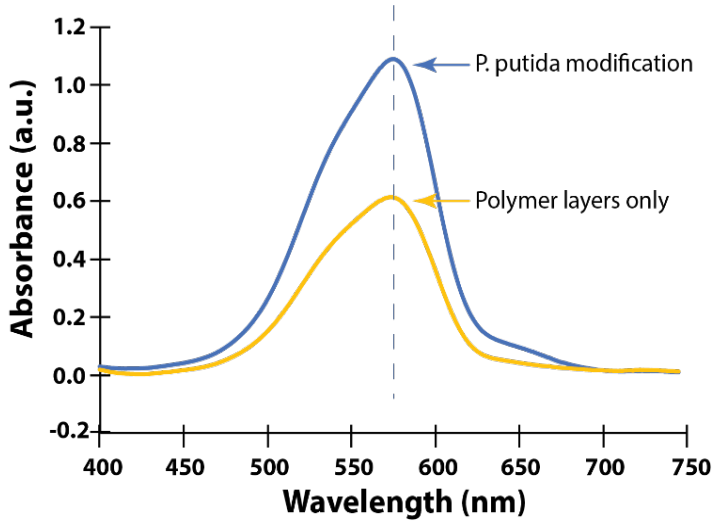

Figure 3.1. UV scan of resulting crystal violet extract from denoted modified electrodes. The blue line demonstrates the CV from P. putida modified electrodes where the yellow line shows electrodes featuring only PDDA/PSS polymer layers.

P. putida biofilm has been shown to be primarily composed of various proteins, polysaccharides, and DNA.[1] Biofilms, in general, allow bacteria such as *P. putida* to form colonies that adhere various surfaces such as glass and metal along with other hydrophilic polar surfaces.[2] These biofilms are typically negatively charged and grow within minutes after a surface is exposed biofilm producing bacteria.[3] While LbL provides a modified electrode that features a mixing of layers, the outer polymer layer, PDDA, is a positively charged and has been shown to foster biofilm adherence in *P. aeruginosa,*[4] which is why we followed a similar preparation protocol for the *P. putida* immobilization strategy here.

Figure 3.1 shows the visible absorbance spectra of a modified biofilm assay to determine if biofilm is grown on the electrode surface. LbL modified electrodes with or without bacteria were exposed to crystal violet (CV) that has been shown to bind within the bacterial biofilm matrix. The CV was extracted following exposure to 35% acetic acid, and the absorbance of the resulting solution was obtained. While some CV does bind within the polymer layers likely based on electrostatic interaction as shown in the yellow line plot in the figure, significantly more absorbance at 575 nm was seen from electrodes featuring *P. putida* growth.

The increased visible absorbance from CV provides evidence that *P. putida* bacteria growth and subsequent biofilm production occurs on the polymer-modified electrode surface. Overall, this shows that the electrodes feature immobilized bacteria for subsequent electrochemical studies.

3.2 Methylene Blue Equilibration

Methylene blue (MB^+) was chosen as the electroactive reporter to assay the poly-P accumulation within *P. putida*. As the electrodes are removed from nutrient broth to buffer, the bacteria on the electrode and the underlying polymers change their structure and growth conditions. This can be seen with the accumulation of MB^+ over time as monitored by SWV. Figure 3.2 shows a SWV overlay monitoring MB^+ accumulation over 2 hr. The data in Figure 3.2a features raw SWV plots that equilibrate over this time to achieve a stable baseline. MB^+ is

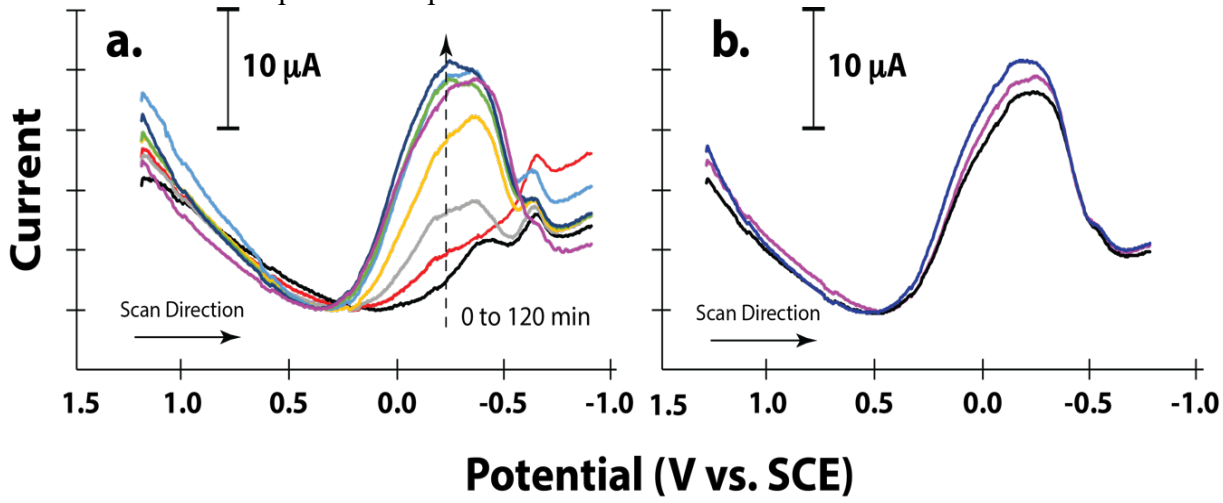

Figure 3.2. a Normalized raw SWV plot overlay showing P. putida modified electrode response over time in a solution of 1 µM MB^+ over 2 hr. b. The 120 min. SWV overlay from three separate P. putida modified electrodes exposed to the same conditions.

cationic and will associate with negatively charged species on the electrode surface, so at this point, its purpose is simply to show that the electrode surface structure is stabilized. This

stabilization is noted as the SWV plots are relatively unchanged starting at around 60 min exposure to MB^+ (cyan plot in Figure 3.2a). Figure 3.2b shows that the electrode surface can be prepared in a reproducible fashion. The figure shows the overlay of the 120 min SWV plots from three separate electrodes that all feature peak currents at ~-0.3 V vs. SCE within +/-10% of each other.

3.3 Poly-P Assay

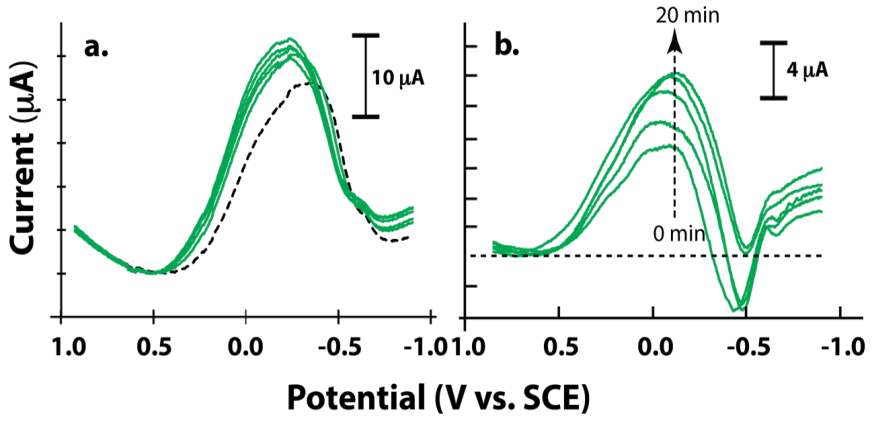

Figure 3.3. a. Normalized raw SWV overlay showing MB^+ response after exposure to 100 µM PO_4^{3-} over 20 min (green) compared to the baseline response (dashed line). b. Baseline corrected response showing difference currents after subtracting out MB^+ response at t = 0 min from subsequent timed runs up to t =20 min.

After allowing MB^+ to equilibrate on the electrode surface and demonstrating that the electrodes could be constructed in a reproducible manner, phosphate was added to the solution and the MB^+ response was monitored over time. Figure 3.3 shows the representative raw SWV response for a *P. putida* modified electrode exposed to 100 µM PO_4^{3-} over 20 min (green scans) compared to the equilibrated MB^+ response (dashed black). This phosphate concentration and the range studied (see below) were chosen because this corresponds to everyday WWTP monitored concentrations. The raw SWV overlay shows that the addition of phosphate caused both the increase in MB^+ amount at the electrode surface based on notable increases in current but also positive potential reduction current shifts as well.

To visualize the current difference over time due to PO_4^{3-} addition, the initial SWV before any phosphate addition (dashed black) was subtracted from subsequent SWV (green). The resulting difference SWV overlay is shown in Figure 3.3b. This difference technique allows for the changes at specific potentials to be more easily visualized. Specifically, upon adding PO_4^{3-} there is an increase in current at ~ -0.1 V with the concurrent decrease at ~ -0.4 V vs. SCE. This suggests that the MB^+ is not only accumulating at the electrode based on overall increases in current, but also changes its bound environment at the electrode surface, the importance of which will be discussed further below.

Several SWV were acquired throughout 2 hr to determine where the MB^+ reduction response saturates. Figure 3.4 plots the peak reduction difference current (ΔI_p) at -0.1V potential from the baseline corrected voltammograms (n=3) at specific time points (t = 0 - 120 min). The plot shows that the MB^+ reduction current after addition of phosphate peaks at approximately 20 min before remaining relatively unchanged. This current plateau suggests that the phosphate related bacterial process has reached its maximum response over the monitored time. Based on these data, 20 min was selected as a sufficient time to monitor the phosphate response on bacteria-modified electrodes.

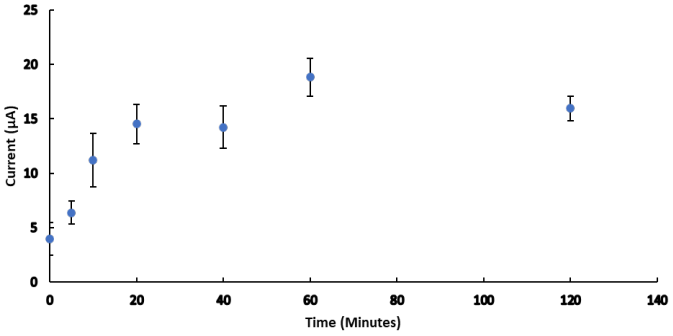

Figure 3.4. MB^+ difference peak currents at -0.1 V vs. SCE as a function of time on P. putida modified electrodes after 100uM PO_4^{3-} exposure. Error bars represent s.d. for n = 3 electrode trials.

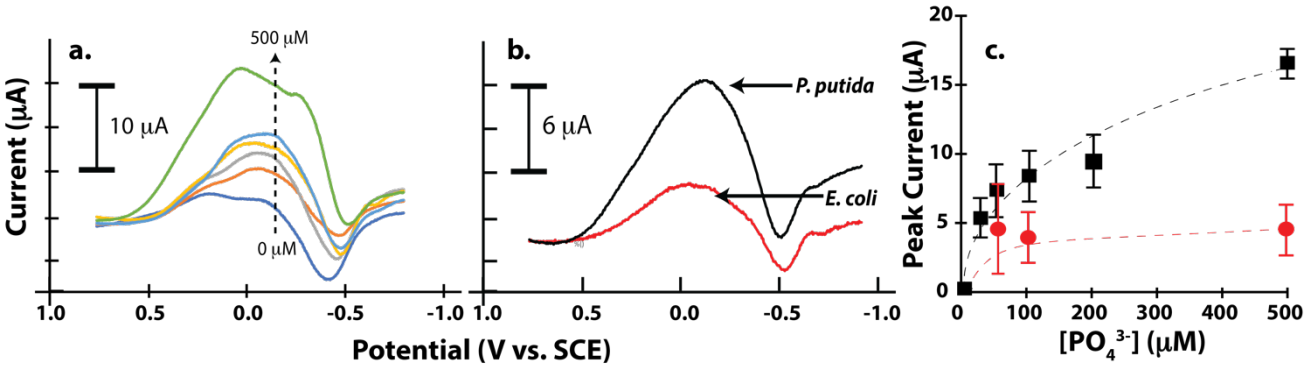

Figure 3.5. a. Difference SWV plot overlay showing MB^+ reduction changes at 20 min at P. putida modified electrodes in the presence of increasing concentrations of PO_4^{3-}. b. 20 min difference SWV comparison between P. putida and E. coli modified electrodes exposed to 100 µM PO_4^{3-}. c. Peak reduction current at -0.1 V as a function of PO_4^{3-} concentration at P. putida (black squares) or E. coli (red circles) modified electrodes. Error bars represent s.d. for n = 3 electrode trials.

The representative MB^+ reduction response dependence on PO_4^{3-} concentration at 20 min phosphate exposure is shown in Figure 3.5a. These data show that the current response increases as a function of phosphate concentration, which suggests that there is an increase of MB^+ on the electrode surface driven by higher concentrations of soluble PO_4^{3-} present. The accumulation of MB^+ would be consistent with poly-P accumulation within the surface bound bacteria due to an increase in soluble PO_4^{3-} exposed to the bacteria. Additionally, the difference SWVs suggest that there are multiple bound populations, which becomes prevalent at higher phosphate exposure concentrations.

The two main populations are at +0.2 and -0.1 V vs. SCE. The emergence of the more positive potential shifted population suggests that the reduced MB^0 is more stabilized in that particular environment vs. the more negative shifted population by ~ 29 kJ/mol based on

$$\Delta G = -nFE$$

where n is the number of electrons transferred to methylene blue (1), F is Faraday's constant (9.65×10^4 C (mol e^-)$^{-1}$), and E is the difference in the two reduction potentials). This suggests a

different binding mode versus a the primarily electrostatic interaction driven environment that would stabilize the oxidized MB^+ form. The importance of these data is discussed below.

The peak current at -0.1 V at 20 min was plotted as a function of PO_4^{3-} concentration and is shown in Figure 3.5c. The plot shows that the accumulation of phosphate possibly reaches a plateau around 200 μM exposure, but it appears that even at 500 μM exposure, the MB^+ currents still increase suggesting that higher phosphate exposure concentrations drive more MB^+ to the *P. putida* modified electrode surface.

Figure 3.5b shows a control baseline corrected SWV comparison of the MB^+ response after 100 μM PO_4^{3-} exposure to *P. putida* and *E. coli* modified electrodes. The purpose of this comparison was to show the difference in response between what is known as a true PAO vs. other bacteria that do not necessarily perform this function. To this end, a separate culture of *E. coli*, a non-PAO, was grown on the PDDA/PSS modified cathode electrodes. These electrodes were equilibrated in1μM MB^+ for 2 hr, similarly to *P. putida* modified electrodes. Figure 3.6 demonstrates a normalized MB^+ equilibrated raw SWV overlay at these electrodes. The overall raw responses are similar to *P. putida* modified electrodes in that the MB^+ takes some time to equilibrate. .

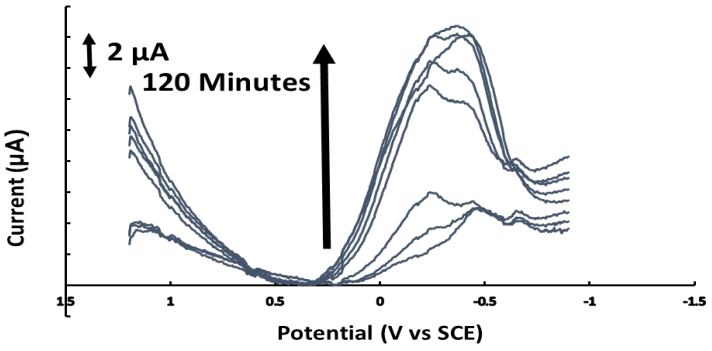

Figure 3.6. SWV overlay showing equilibration of 1 μM MB^+ on E. coli modified electrodes over 2 hr.

The electrochemical responses at *E. coli* modified electrodes differ from those at *P. putida* modified electrodes upon exposure to selected concentrations of PO_4^3 mainly in the

intensity of current generated. This can be seen in the aforementioned SWV comparison in Figure 3.5b and the overall difference peak current plots in Figure 3.5c showing that the MB^+ reduction peak currents reach a maximum in the presence of *E. coli* at much lower concentrations of phosphate exposure. The lower current increases suggest that the phosphate-related bacteria processes at the electrode surface reach a level of completion, and higher concentrations of soluble phosphate do not affect the bacteria and the resulting MB^+ binding environment. Overall, this control shows that the MB^+ related electrochemical changes that occur upon phosphate exposure are much more prevalent in the presence of *P. putida* vs. *E. coli* on the electrode surface, which is consistent with the PAO functionality of the former bacteria.

3.4 Extended Time Trials

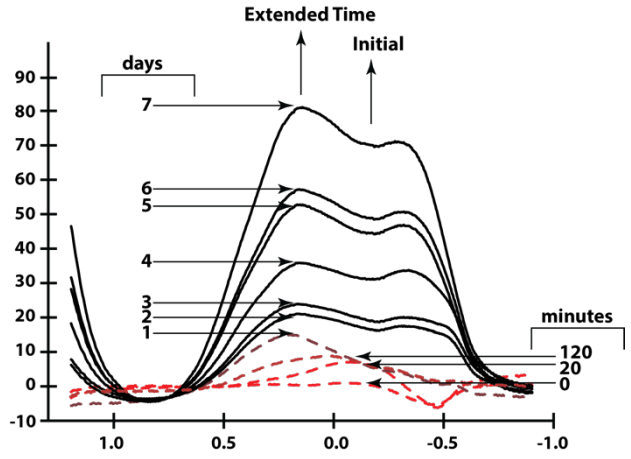

Figure 3.7. Baseline corrected MB^+ SWV response upon 100 µM of PO_4^{3-} exposure to P. putida modified electrodes over the course of 7 days. Current increases at initial time and extended time are denoted with the arrows.

Figure 3.7 shows the background subtracted SWV results when a *P. putida* modified electrode was exposed to PO_4^{3-} for up to seven days. The figure shows that the electrochemical response shows the reduction of MB^+ within multiple environments over this time period. Initially, the current at -0.1 V increases and saturates at around 20 mins (red dashed responses), as explained previously, before increasing at approximately +0.2 V over the course of the study. The current increase at this positive shifted potential is delayed, consistent with what might be expected for poly-P storage; however, this line of experiments to confirm this was not explored.

3.5 Relevant Media Controls

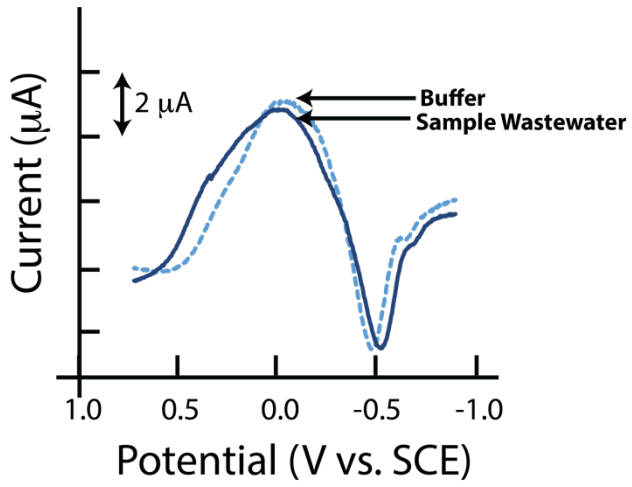

Figure 3.8. Baseline corrected MB^+ SWV comparison response upon 100 µM of PO_4^{3-} exposure to P. putida modified electrodes in E-buffer and WWTP model water denoted with the arrows.

Real-world wastewater contains a wide range of ions, such as nitrates, carbonates, and ammonium.[6] In addition, the ion concentrations vary from day to day and season to season as changing weather patterns such as rain and drought will affect total water into the WWTP. [6,] These ions have the potential to alter cellular biofilms. Calcium for example has been shown to increase the biofilm accumulation rate.[7, 8] Salts such as sodium chloride can reduce viscosity and adhesion of biofilms.[9] To determine how a more accurate water model would affect the sensing aspects of the bacteria-modified electrodes, similar electrochemical experiments utilizing the MB^+ equilibrated *P. putida* electrodes exposed to phosphate were performed in a solution made with several salts based on GUC wastewater data. Figure 3.7 shows a baseline corrected SWV comparison demonstrating the differential electrochemical response between two representative trials where 100 µM PO_4^{3-} was exposed to the modified electrodes, one in E-buffer and one in WWTP model solution.

The figure shows that the response is generally very similar. The magnitude of current increase as well as the location of MB^+ reduction potentials remain the same between the two solutions, which demonstrates that the WWTP solution does not alter the bacteria or electrode

environment sufficiently to preclude the monitoring of MB^+ as the electrochemical probe. Similarly, the inclusion of polyvalent cationic salts (e.g. Ca^{2+}) does not seem to affect the adsorption of MB^+ on the electrode surface upon phosphate exposure. This is meaningful as the attraction of higher valent salts should out-compete and preclude any attraction and interaction of monovalent counterions to the surface, such as MB^+, but also, the solubility product constant (K_{sp}) of $Ca_3(PO_4)_2$ is very low (~10^{-33}), suggesting that a precipitate may form with phosphate exposure which could block electron transfer. These data show that these situations did not occur or limit the sensing aspects of the bacteria-modified electrode.

3.6 Temperature Effects

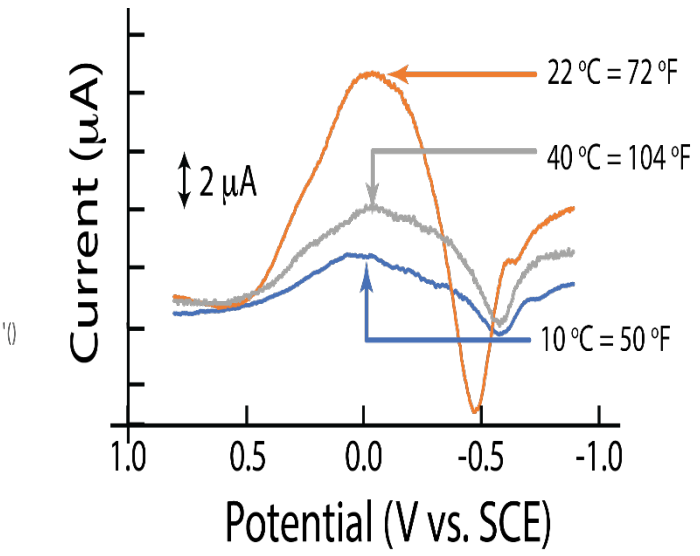

Figure 3.9. SWV difference plot comparing 100 µM of PO_4^{3-} on MB+ equilibrated bacteria modified electrodes in E-buffer solution at a range of temperatures, 40 ºC (Grey), 22 ºC (Orange) and 10 ºC (Blue)

The electrochemical response at a variety of temperatures needs to establish the ability of the sensor to operate in situations that more accurately mirror outdoor weather that can be expected locally. *P. putida* shows optimal growth and activity around 30ºC [11, 12] while growth and activity slow at temperatures higher than 35 ºC [11] and lower than 10 ºC.[12] *P. putida* loses function at temperatures as high as 40 ºC [11] and as low as 4 ºC.[12]

Cellular function reduces and eventually ceases with these temperature changes so this would impact the accumulation of poly-P. Higher temperatures also affect dissolved oxygen content while lowering the temperature impacts this in the opposite direction.[13] Since poly-P

accumulation is dependent on oxygen levels, the effects of high temperature can have a significant effect on PAO activity. Indeed, the summer months are the most problematic for GUC, and likely all similarly operated WWTP, in terms of biological phosphate remediation.

Figure 3.8 shows the SWV overlay of the MB^+ response when *P. putida* modified electrodes were exposed to 100µM PO_4^{3-} at the denoted temperatures. The figure shows how the response is muted somewhat at temperatures outside of the optimal window. However, two important aspects should be noted regarding this data. First, the responses are still registering above baseline, and the current response is higher at the elevated temperature condition vs. the lower condition. This is important as it is well-documented that the hot summer months impact the EBPR process more than the colder ones. This suggests that the current responses are still viable, and the sensor could be utilized at these conditions. Second, this shows that the current responses are a bacteria driven vs. a non-specific charge compensation driven process. If the MB^+ response was merely due to the addition of anionic phosphate and the subsequent association of some sort of charge complex at the electrode, temperature should impact that process very little. The large current difference obtained as conditions drift from room temperature suggests that the current obtained at the electrode surface is based on the activity of the bacteria immobilized on the electrode surface upon exposure to conditions that vary from those that are more optimal.

3.7 Discussion of Electrochemical Results

The electrochemical assay demonstrates the relative change in the MB^+ environment upon addition of addition of PO_4^{3-}. This change is established by allowing the MB^+ to equilibrate on the bacteria modified surface before any phosphate is exposed to the electrode and the

immobilized bacteria. Therefore, it was first necessary to establish that bacteria were bound on the electrode to show that these subsequent MB^+ electrochemical changes were indeed due to bacteria processes upon exposure to PO_4^{3-}.

To this end, several data sets are consistent with bacteria present on the electrode surface. First, the CV assay showed an almost a 100% absorbance increase upon exposure of CV to a *P. putida* modified electrode vs. one that was only modified with the underlying polymer layers. CV has been shown to bind within the bacterial biofilm matrix; therefore, the absorbance increase based on the increased concentration of CV present on the electrode surface after exposure to *P. putida* is consistent with the presence of biofilm forming bacteria immobilized on the electrode surface. Second, while not necessarily the primary reason for performing the temperature dependence study, the decrease in MB^+ reduction changes upon PO_4^{3-} addition as the temperature is varied is consistent with a bacterial process occurring on the electrode as the bacteria do not operate as optimally at temperatures removed from their optimal conditions. If this was a non-specific process – i.e. PO_4^{3-} driving cationic MB^+ to the electrode surface, temperature would likely not play such a drastic role.

With evidence suggesting that the electrode was successfully modified with *P. putida* (or *E. coli*), this suggests that the changes in MB^+ reduction as denoted in Figure 3.3 are due to the phosphate-related bacteria processes upon the addition of soluble PO_4^{3-} to the solution – namely the PAO activity of *P. putida*. Before PO_4^{3-} exposure, MB^+ binds to the bacteria-modified surface, likely at anionic sites within the bacteria or underlying PSS layers. Upon exposure, the *P. putida* are known to uptake added soluble PO_4^{3-}, converting the individual ortho units into additional long and short form poly-P structures. As these develop and grow, this creates

additional sites where MB^+ can bind. Additional binding sites, or an additional binding environment, is detected upon MB^+ reduction generating an increase in current at potentials that drift from the initial reduction potential (the formal potential, E^f). Reduction at potentials that vary from the initial E^f suggest the stabilization of either the reduced (if the new reduction potential is negative shifted from E^f) or oxidized (if the new reduction potential is positive shifted from E^f) form of the molecule on the electrode surface. This is likely due to additional intermolecular interactions present.

Figures 3.3 and 3.5 show positive shifts in the MB^+ reduction potential with PO_4^{3-} addition, suggesting that the oxidized MB^0 form is stabilized. Previous research utilizing 4-4'-bipyridyl (viologen) compounds showed similar reduction potential shifts as the molecules were able to engage in more hydrophobic intermolecular interactions at critical concentrations on an electrode.[14, 15] A similar situation may be present here as the MB^+ structure likely engages in additional interactions based on the affinity for the poly-P structure. A speculative complex may be the association of the molecule between the phosphate units upon reduction. Additionally, based on the data of Figure 3.5a, it appears that MB^+ bonds at several environments based on the emergence of multiple reduction potentials.

Nonetheless, the shifts in reduction potential suggest a change in the MB^+ binding environment due to phosphate-related processes occurring within the PAO bacteria as Figure 3.5b-c demonstrate the difference between *P. putida* and *E. coli* after exposure to PO_4^{3-}. Responses at either *E. coli* or *P. putida* were similar, albeit with much lower current changes at *E. coli*. This equates to less MB^+ present at that bacteria surface following the generation of the baseline response, which is consistent with the diminished PAO process these bacteria are known

to undergo vs. *P. putida*.[5] This is even more pronounced at higher phosphate concentrations, where current changes at *P. putida* electrodes are significantly higher than those at *E. coli* (Figure 3. 5c).

The use of *P. putida* shows a much higher current response change upon the reduction of MB^+ after exposing the electrode to PO_4^{3-}. Charting the peak currents at a specific potential (-0.1 V for Figures 3.4 and 3.5c) allows for the use of this sensor approach to determine the efficacy of PAO activity in a solution. Based on the preliminary data here using a model wastewater solution in terms of ion content, it appears that this sensor approach shows promise in this area as MB^+ current change responses were similar in either buffer or the model solution (Figure 3.7). Also, it appears that the sensor can still be operated at different environmental conditions showing how the bacteria might be affected at different temperatures (Figure 3.8). How might this look at a WWTP? A hypothetical scenario would involve a pre-MB^+ loaded sensor inserted into the treatment basin with periodic SWV acquisitions. Software treatment of the SWV would indicate the increase in current at specific potentials as phosphate in the wastewater is exposed to the electrode surface, which would indicate the health of the PAO bacteria in the basin.

Overall, this electrochemical biosensor can detect a change in the methylene blue binding environment within the immobilized bacteria on the surface of carbon electrodes. The sensors show a dependence on PO_4^{3-} exposure time and concentration and a on temperature, which are consistent with PAO activity of the surface bound bacteria. They appear to be robust enough to monitor the process at conditions comparable to those seen at the WWTP. The further development of these sensors would represent a powerful tool in monitoring the functionality and health of PAO at WWTP facilities.

References

(1) Jahn A, Griebe T, Nielsen, PH. *Composition of pseudomonas putida biofilms: Accumulation of protein in the biofilm matrix*. Biofouling, 1999,14(1), 49–57. DOI: 10.1080/08927019909378396

(2) Donlan RM. *Biofilms: microbial life on surfaces*. Emerg Infect Dis. 2002,9,881-90. DOI: 10.3201/eid0809.020063.

(3) Loeb GI, Neihof, RA. *Marine Conditioning Films. In Advances in Chemistry: Vol. 145. Applied Chemistry at Protein Interfaces*, 1975, 319–335. DOI: 10.1021/ba-1975-0145.ch016

(4) Robb, AJ, Vinogradov S, Danell AS, Anderson E, Blackledge MS, Melander C, Hvastkovs EG. *Electrochemical detection of small molecule induced Pseudomonas aeruginosa biofilm dispersion*, Electrochimica Acta, 2018, 268, 276-282. DOI: 10.1016/j.electacta.2018.02.113

(5) Rao NN, Liu S, Kornberg A. *Inorganic polyphosphate in Escherichia coli: the phosphate regulon and the stringent response*. J Bacteriol. 1998, 180(8),2186-93. DOI: 10.1128/JB.180.8.2186-2193

(6) Henze M, Loosdrecht M, Ekama G, Brdjanovic D. *Biological Wastewater Treatment: Principles,* Modeling and Design. 2008. DOI: 10.2166/9781780408613.

(7) Turakhia MH, Characklis WG. *Activity of Pseudomonas aeruginosa in biofilms: effect of calcium*. Biotechnol Bioeng. 1989, 33(4),406-14. DOI: 10.1002/bit.260330405. PMID: 18587931.

(8) Chen X, Stewart, PS. *Role of electrostatic interactions in cohesion of bacterial biofilms.* Appl Microbiol Biotechnol. 2002 59, 718–720. DOI: 10.1007/s00253-002-1044-2.

(9) Gordon CA, Hodges NA, Marriott C. *Use of slime dispersants to promote antibiotic penetration through the extracellular polysaccharide of mucoid Pseudomonas aeruginosa*. Antimicrob Agents Chemother. 1991,35(6), 1258-60. DOI: 10.1128/AAC.35.6.1258.

(10) Butcher JB, Covington S. *Dissolved-Oxygen Analysis with Temperature Dependence. Journal of Environmental Engineering*, 1995, 121(10), 756–759. DOI:10.1061/(ASCE)0733-9372(1995)121:10(756).

(11) Munna, MS, Zeba Z, Noor R. *Influence of temperature on the growth of Pseudomonas putida*. Stamford Journal of Microbiology. 2016, 5. 9. DOI: 10.3329/sjm.v5i1.26912.

(12) Fonseca P, Moreno R, Rojo F. *Growth of Pseudomonas putida at low temperature: global transcriptomic and proteomic analyses*. Environmental Microbiology Reports, 2011, 3, 329-339. DOI: 10.1111/j.1758-2229.2010.00229.x.

(13) Butcher JB, Covington S. *Dissolved-Oxygen Analysis with Temperature Dependence. Journal of Environmental Engineering*, 1995, 121(10), 756–759. DOI: 10.1061/(ASCE)0733-9372(1995)121:10(756).

(14) Satterwhite JE, Pugh AM, Danell AS, Hvastkovs EG. *Electrochemical detection of anti-benzo[a]pyrene diol epoxide DNA damage on TP53 codon 273 oligomers*. Anal Chem. 2011, 83(9), 3327-35. DOI: 10.1021/ac103091v.

(15) Tang X, Schneider TW, Walker JW, Buttry DA. *Dimerized π-Complexes in Self-Assembled Monolayers Containing Viologens: An Origin of Unusual Wave Shapes in the Voltammetry of Monolayers*, Langmuir, 1996, 12(24), 5921-5933. DOI: 10.1021/la9503764.

CHAPTER 4: ICP-MS VALIDATION

4.1 Results

The electrochemical sensor merely reports that the MB^+ electrochemical environment on the electrode surface changes following phosphate exposure. The increasing current presumably involves the poly-P processes by appropriate bacteria, but the signal response must be validated to ensure that poly-P accumulation occurs from these bacterial processes. To this end, ICP-MS was used to validate the bacterial processes, and by extension the electrochemical responses, by monitoring changes in phosphorus (P) following exposure to *P. putida* and *E. coli* in solution.

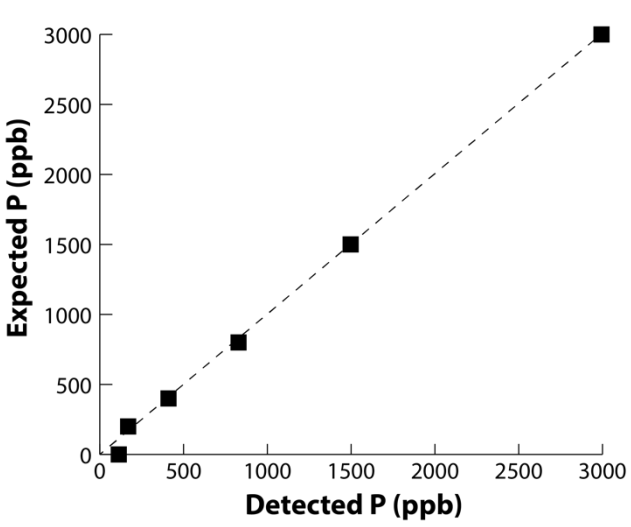

Figure 4.1. ICP-MS calibration showing the expected P concentration vs. actual detected (ppb).

The details of these studies are summarized in Chapter 2, but briefly, the goal was to expose phosphorus in the form of PO_4^{3-} to both forms of bacteria used in this study and determine the P concentrations following this exposure. Decreases in collected P concentrations provide evidence that the bacterial processes occur in the manner described, and that the electrode processes and observed current changes were due to poly-P accumulation.

The calibration of the instrument was established via dilution of purchased standards. The instrument was able to detect P in a range from 0-3000 ppb with only minimal deviation from the expected concentrations as seen in the Figure 4.1 plot. The instrument does detect P more

accurately at higher concentrations as the blank did register a concentration of 109(±35) ppb. This RSD error decreased from 15% to 0.2% as the concentrations increased. This is likely due to possible erroneous phosphate introduction due to its ubiquity or possible limitations in the detection of P at lower concentrations, which is an ICP-MS limitation for this element. However, at higher concentrations the deviation from expected P concentration averaged only 15 ppb, which shows that the calibration was useful.

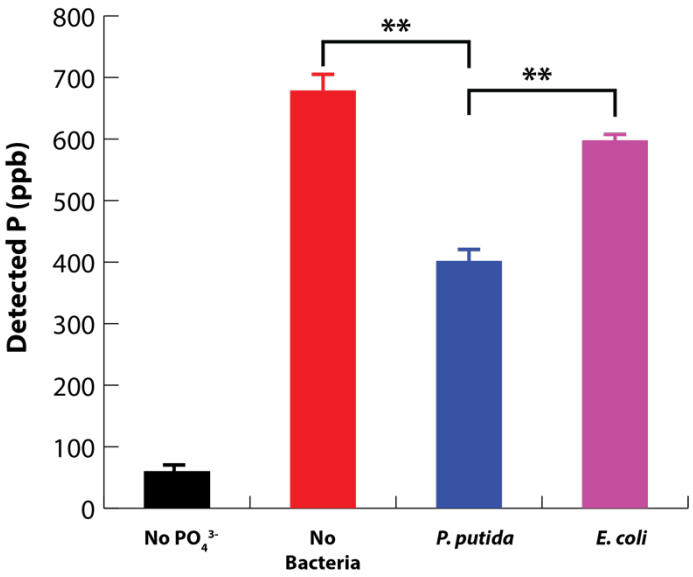

Figure 4.2. Detected P (ppb) from each denoted sample. No PO_4^{3-} sample included P. putida, all other bacterial samples were exposed to the same PO_4^{3-} concentration before dilution. Error bars denote s.d. for n = 2; asterisk denotes statistical significance (p < 0.002).

Remaining samples included the bacterial trials and controls. Here, bacteria were first grown then starved of O_2 before reaeration and exposure to phosphate. The bacteria were allowed to incubate with the phosphate before centrifugal filtration to remove the high molecular weight species (i.e. bacteria) and collect the remaining phosphate solution to determine the P concentration. The results from these analyses are shown in the plot of Figure 4.2. The data show a statistically significant decrease ($p < 0.002$) in detected P from *P. putida* samples by roughly 200 ppb compared samples without bacteria or those containing *E. coli*. No statistical significance was determined between *E. coli* and 'no bacteria' samples despite those containing *E. coli* exhibiting lower detected P. Lower concentrations here may denote some poly-P

accumulation or other cellular process by *E. coli*, but at a significantly lower amount compared to *P. putida*.

One experimental procedure that was necessary to manifest the detected decrease in P between the bacteria was to remove O_2 (via Ar purge) before reaeration. Comparing these data to experiments where the samples were treated with these conditions, *P. putida* and *E. coli* PO_4^{3-} exposed samples generated the same levels of detected P where the average difference between samples was 3 ppb following phosphate exposure and filtration.

4.2 Discussion

ICP-MS data shows a loss in P from samples containing *P. putida* and to a lesser extent *E. coli* compared to samples without any bacteria present. This loss of P from the addition of PO_4^{3-} to the solution correlates with likely cell growth as well as poly-P accumulation in the form of luxury phosphorous uptake. Both processes occur in an oxygenated PO_4^{3-} rich environment with poly-P accumulation occurring before cell growth occurs.[1]

The change in P concentration as a product of poly-P accumulation and cell growth would explain the significant loss of P from *P. putida* samples. *E. coli* has been shown to accumulate poly-P to a much lesser extent than *P. putida*.[2] These bacteria undergo similar processes where upon anaerobic stress, they release PO_4^{3-} followed by luxury P uptake upon reexposure to aerobic conditions.[3,4] However, after reaching poly-P conversion activity saturation, the bacteria engage in cell growth.[1] *E. coli* colonies possess a faster cell doubling time compared to *P. putida*, approximately 20 min compared to 40-50 min for *P. putida.*[5,6] Bacterial growth necessitates PO_4^{3-} for cellular structures, which is similar to population explosions seen in phosphorous rich water systems.[1] Considering their reported cell growth rates, if *P. putida*

used P solely for cellular growth, a higher remaining P concentration compared to *E. coli* samples would be expected after bacteria exposure. However, the significant decrease of P from *P. putida* suggests a secondary P accumulation, which is strong evidence for poly-P accumulation within these bacteria.

Based on these results, *P. putida* engages in poly-P accumulation, whereas *E. coli* essentially does not. Weaving these data into the electrochemical narrative, this provides strong evidence that the increasing currents seen on *P. putida* modified electrodes are due to poly-P accumulation from these bacteria. The significantly muted *E. coli* current increases could be due to some poly-P accumulation, which is in line with the ICP-MS results here showing that *E. coli* does not consume as much P. The only potential issue between the data sets could be the use of Ar/O_2 purging for solution phase ICP-MS studies vs. stirring only for electrochemical sensor acquisitions. However, it is known that the LbL-modified electrode surface is highly concentrated with reagents and, in this case bacteria, compared to the analogous solution-phase chemistry. This has manifested itself in significantly elevated reaction kinetic rates for chemical and enzymatic reactions that cannot be envisioned without electrode immobilization.[8] While we certainly need to perform more experiments to confirm this, the LbL surface modification, which creates a vastly different environment vs. those in a centrifuge tube likely influences the conditions to give rise to poly-P accumulation and the resulting different electrochemical responses between the two bacteria.

Overall ICP-MS provides the means to show that P. putida definitively sequesters P (from xenobiotic PO_4^{3-} exposure) as compared to control *E. coli* bacteria. This process is facilitated via establishing anaerobic conditions before O_2 exposure, in line with the known

cellular process. Taken together, ICP-MS results demonstrate that the electrochemical sensor current output does reflect poly-P accumulation by surface immobilized bactera.

References

(1) Tarayre C, Nguyen HT, Brognaux A, Delepierre A, De Clercq L, Charlier R, Michels E, Meers E, Delvigne F. *Characterization of Phosphate Accumulating Organisms and Techniques for Polyphosphate Detection: A Review*. Sensors, 2016,16(6), 797. doi: 10.3390/s16060797.

(2) Saia SM, Carrick HJ, Buda AR, Regan JR, Walter TM. *Critical Review of Polyphosphate and Polyphosphate Accumulating Organisms for Agricultural Water Quality Management*. Environmental Science & Technology, 2021, 55 (5), 2722-2742. doi: 10.1021/acs.est.0c03566.

(3) Lopez-Vazquez CM, Oehmen A, Hooijmans CM, Brdjanovic D, Gijzen HJ, Yuan Z, van Loosdrecht MCM. *Modeling the PAO–GAO competition: Effects of carbon source, pH and temperature*. Water Research, 2009, 43(2),450–462. doi: 10.1016/J.WATRES.2008.10.032

(4) Rao NN, Liu S, Kornberg A. *Inorganic polyphosphate in Escherichia coli: the phosphate regulon and the stringent response*. J Bacteriol, 1998, 180(8), 2186-93. doi: 10.1128/JB.180.8.2186-2193.1998.

(5) Gibson B, Wilson DJ, Feil E, Eyre-Walker A. *The distribution of bacterial doubling times in the wild.* Proc Biol Sci, 2018, 285(1880), 20180789. doi: 10.1098/rspb.2018.0789.

(6) Fonseca P, Moreno R, Rojo F. *Growth of Pseudomonas putida at low temperature: global transcriptomic and proteomic analyses.* Environmental Microbiology Reports, 2011, 3, 329-339. doi:10.1111/j.1758-2229.2010.00229.x.

(7) Yuste L, Canosa I, Rojo F. *Carbon-Source-Dependent Expression of the PalkB Promoter from the Pseudomonas oleovorans Alkane Degradation Pathway*. Journal of bacteriology, 1998, 180, 5218-26. doi: 10.1128/JB.180.19.5218-5226.1998.

(8) Hvastkovs EG, Rusling JF. *State-of-the-Art Metabolic Toxicity Screening and Pathway Evaluation*. Analytical Chemistry, 2016, 88, 4584-4599.

CHAPTER 5: CONCLUSIONS AND FUTURE OUTLOOK

These previous chapters have laid out a series of experiments that have provided the groundwork for the development of a biosensor to detect the accumulation of poly-P within PAO to provide insight on the health of enhanced biological phosphate treatment in a WWTP. Following established LbL protocols, *P. putida* was grown and immobilized on graphite electrodes. Following exposure to PO_4^{3-}, electroactive MB^+ was used as an indirect means to assay the changes in the bacteria due to phosphate exposure. Cationic, small molecule MB^+ penetrates within the biofilm and bacterial cells to associate with the formed poly-P. SWV reduction of the MB^+ shows that currents increase as a function of PO_4^{3-} concentration and bacteria present. The currents essentially plateau after 20 mins, showing that this sensor can detect these bacterial processes rather quickly.

The electrochemical response was very similar in model wastewater as the sensor was able to detect current changes in the presence of several ionic interferences. Additionally, the sensor was able to detect current changes from PO_4^{3-} exposure at a range of temperatures. The main issue for WWTP facilities is determining if the EBPR process is operating at sufficient efficiency in the hot summer months. While the signals were muted at higher temperatures as the bacteria undoubtedly become stressed, the sensor was able to determine activity via MB^+ current changes.

Finally, the electrochemical sensor only reports changes in MB^+ binding environment – by itself, it does not actually provide definitive information about the cellular process. Additional analytical techniques must be employed to validate the presumed processes occurring on the electrode surface to provide meaning to these current changes. To this end, ICP-MS

studies measuring the loss of P over exposure to both *P. putida* and *E. coli* showed that *P. putida* did in fact sequester substantially more P than *E. coli* over the exposure time. This is even more remarkable as the growth rate for *P. putida* is significantly slower; therefore, this shows that these bacteria are likely sequestering this P as poly-P. Coupled with the electrochemical results, this evidence shows that the large MB^+ current increases upon PO_4^{3-} exposure to *P. putida* are due to these bacteria sequestering poly-P, which changes the MB^+ binding environment within the films. Slight changes in binding environment lead to thermodynamically altered states, which lead to slight changes in reduction potential, which is exactly what we see here.

Work on the biosensor project will continue, and several questions still must be answered. Is *P. putida* the best model bacteria to use? This bacterium was chosen due to its ease in handling and growth protocols. However, other bacteria might exhibit improved poly-P accumulation abilities, which would generate larger currents. Other bacteria might be better to model the hotter weather conditions, which might show that the EBPR process is efficiently operating and be of more use in WWTP settings. Also, there are several other experimental parameters that might be employed to optimize this sensor. For instance, purging with Ar to model anaerobic conditions before O_2 purging to model aerobic conditions significantly altered the solution-phase bacterial processes. This may not have any impact on immobilized bacteria, but these are a series of studies that need to be conducted. Also, it is possible different buffer solutions or model solutions may produce better conditions for the sensor to operate. These studies do take a significant amount of time to complete. Finally, the ultimate use of this sensor would be at a WWTP, like GUC, and steps to implement this approach either with water obtained from the facility or at the facility itself are currently underway.